

## Effect of Sr<sup>2+</sup> doping on the structural and dielectric properties of BaTiO<sub>3</sub> lead free piezoelectric ceramics

Samar.B.Moeen, Abd El-razek Mahmoud, M.K.Gerges

Physics Department, Faculty of Science, South Valley University, Qena 83523, Egypt

**Abstract:** In order to investigate effect of Sr ions on the structural and dielectric properties of BaTiO<sub>3</sub>, a series of (Ba<sub>1-x</sub>Sr<sub>x</sub>)TiO<sub>3</sub> (x=0.0, 0.05, 0.1, 0.2 and 0.4mol%) were prepared by Sol gel method. The calcination and sintering temperatures were carried out at 1000°C and 1200°C respectively for 2h. To evaluate the functional groups of the BST calcined powders, FT-IR has been used. The structure and phase identification were identified by X ray diffraction (XRD), and all the peaks were indexed by BT (tetragonal structure P4/mm space group) perovskite structure and no second phases can be observed. In addition to, all the peaks were shifted to the higher degree by increasing Sr amount indicate decreasing the lattice parameters. Morphology and the microstructures of the ceramic compositions were observed by scanning electron microscope (SEM). Dielectric properties and impedance analysis as a function of temperature and frequency for the BST ceramics were investigated.

### I. INTRODUCTION

Ferroelectric materials or ferroelectrics refer to the group of dielectrics having the property of spontaneous polarization (i.e., they retain a dipole even after an applied voltage has been removed). The key characteristics of a ferroelectric crystal are that the direction of the polarization can be reversed by application of an electric field and that a hysteresis loop results. Ferroelectrics mainly have two characteristics, asymmetry and high dielectric constant or high permittivity [1,2]. Barium Titanate (BaTiO<sub>3</sub>) was the first discovered piezoelectric transducer ceramic that satisfied the need of a high dielectric constant material for capacitor application during World War II in the mid 1940s [3]. Addition of ions in BaTiO<sub>3</sub> structure at the A or B site reduces change in electric properties. Based on the transducer application, Sr<sup>2+</sup> is used to reduce T<sub>c</sub> but Ca<sup>2+</sup> has a negligible change in Curie temperature [4,5].

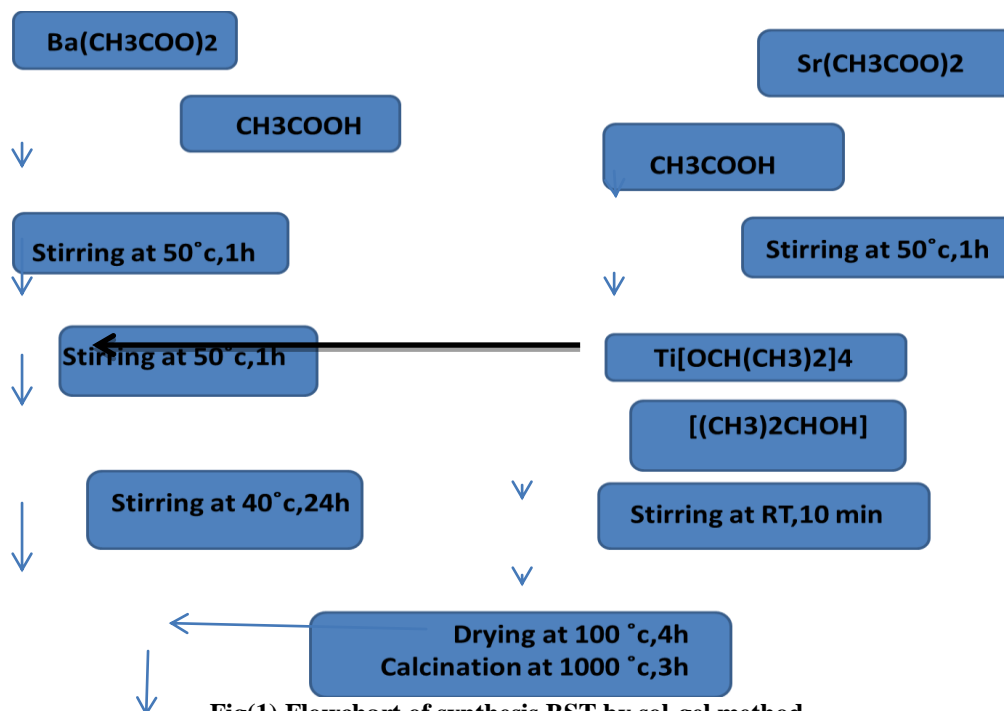
Synthesis method played a significant role in determining the microstructure, electrical and optical properties of ferroelectric ceramics [6,7]. Electrical properties are strongly dependent on the grain size and the crystalline structure [8]. However, chemistry co-precipitation [9], organic acid precursor [10,11], microemulsion [12,13], etc. This paper focused on developing and understanding the synthesis behavior of nanosized barium strontium powders by Sol-gel process.

Strontium-doped barium titanate (BST) has been widely used for various applications, such as fields of electronics and telecommunications, because of its high dielectric constant, large electric field tunabilities, and relatively low dielectric losses [14,15].

### II. EXPERIMENTAL

The perovskite (Ba<sub>1-x</sub>Sr<sub>x</sub>)TiO<sub>3</sub> lead free nano-ceramics (x=0.0, 0.05, 0.1, 0.2 and 0.4mol% of Sr) were synthesized by using Sol-gel technique. Both of barium acetate Ba(CH<sub>3</sub>COO)<sub>2</sub>, strontium acetate Sr(CH<sub>3</sub>COO)<sub>2</sub> and titanium isopropoxide Ti[OCH(CH<sub>3</sub>)<sub>2</sub>]<sub>4</sub> were used as the precursor for obtaining barium, strontium and titanium. Glacial acetic acid (CH<sub>3</sub>COOH) was used as a solvent for barium acetate and calcium acetate, and 2-propanol [(CH<sub>3</sub>)<sub>2</sub>CHOH] was used as a solvent for titanium isopropoxide. Fig.1. shows the flowchart of the sol gel procedures. In the beginning, stoichiometric weight of barium acetate was dissolved in 20ml of acetic acid by using magnetic stirrer at 60°C, for 1 hour, after that stoichiometric proportion of strontium acetate was dissolved in 5ml of acetic acid by magnetic stirrer at 60°C for half an hour. The two separated solutions were mixed and refluxed at 60°C with vigorous stirring for 1h to obtain a transparent solution. At the same time of refluxing, 10ml of 2-propanol was added to the stoichiometric weight of titanium

isopropoxide and kept in magnetic stirrer for half an hour at room temperature. The titanium isopropoxide solution was added to the Ba-Sr solutions, and the all mix was left for 24h at 40°C until to form a thick of white gel of BCT containing organic materials. Finally, the gel was kept in the hot plate and dried at 100°C, for 4h dwell time to obtain amorphous powder of BST. The amorphous powder was calcined at 900°C, for 3h in a covered platinum crucible to avoid any possibility of contamination during the thermal treatment. The calcined powder was grind in a mortar pestle and sieved through 38µm grid to obtain fine single phase powder. Hydraulic pressure was used to form a cylinder pellets with 10mm in diameter and 1.5mm in thickness inside the steel die. The pellets were sintered at 1300°C, 4h and (10°C/min) as heating/cooling rate in the covered platinum crucible in an air. X-ray diffractometre(PANalyticalx'Pert PRO diffractometre) (XRD) with CuK $\alpha$  radiation was used to record the diffraction pattern for both of BCT calcined powder and sintered ceramics at room temperature. The morphology and microstructure of BST calcined powder and ceramics were examined using Scanning electron microscope equipped with an energy-dispersive X-ray (EDS) analyzer (SEM-EDS) (JEOL, JEM-2100 – Japan). Small amount of calcined powder was mixed with (potassium bromide, KBr) and a (Jasco Model 4100 –Japan). was used to identify the IR-active functional group of the present compositions in the wide range of wave number (4000-400cm<sup>-1</sup>). A layer of gold was deposited into the top and bottom surface of the sintered pellets for carried out the dielectric measurements. The dielectric properties for all the sintered ceramics dependant of frequency (100Hz-8MHz) were studied by using (HIOKI 3532-50 LCR HITESTER).P-E loop measured at room temperature by (RADIANT Precision premium II Multiferroic Ferroelectric Test System10 kV HVI-SC-Model609B)



Fig(1) Flowchart of synthesis BST by sol-gel method.

### III. RESULTS AND DISCUSSION

#### 3.1. Characterization of BCT calcined powder:

Fig(2) shows the X-Ray powder diffraction of the powder of B<sub>1-x</sub>S<sub>x</sub>TiO<sub>3</sub> where x=(0.0,0.05,0.1,0.2 and 0.4)mol % of Sr. Sample calcined at 1000°C for 4 h. All samples crystallize in the pure perovskite phase, All the diffraction peaks can be matched with the standard data of (pdf No.0.1-0.75-0.473) and (P4/mm space group) according to the JCPDS database. In addition we note that when the strontium doping rate was increased, the diffraction peaks slightly shift toward higher angles [16]

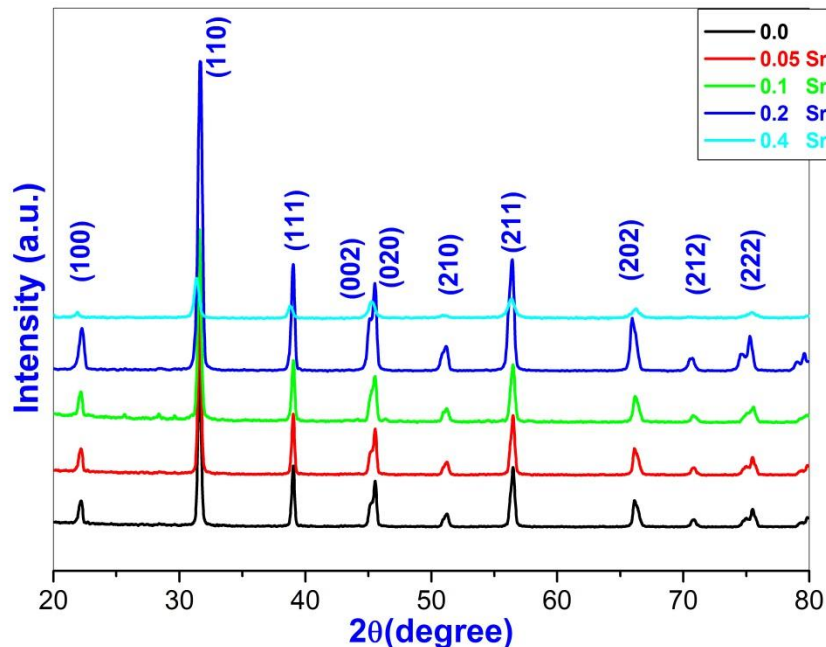
The particle size of the BST calcined powder was calculated by scherrerEq(1)

$$d = 0.94\lambda / \beta \cos\theta$$

where d,  $\lambda$ ,  $\beta$  and  $\theta$  represent the particle size, wavelength of the CuK $\alpha$  radiation ( $\lambda=1.5418^\circ\text{A}$ ), full width at half maximum of peak

Sr doping gives rise to a slight transformation from quadratic (pure BT) to pseudo cubic phase ( $\text{BST}_x, x > 0.2$ ) as revealed by the peak (200) in the range  $44^\circ < 2\theta < 47^\circ$ . These two peaks tend to merge as observed for the three other compositions [17].

In addition, we note that when strontium content increases, the tetragonality of the structure decreases and that for  $x > 0.2$  in Sr, the structure stabilizes in the pseudo cubic one, due to electrostatic repulsions between 3d electrons of  $\text{Ti}^{4+}$  ions and 2p electrons of  $\text{O}^{2-}$  ion [18].



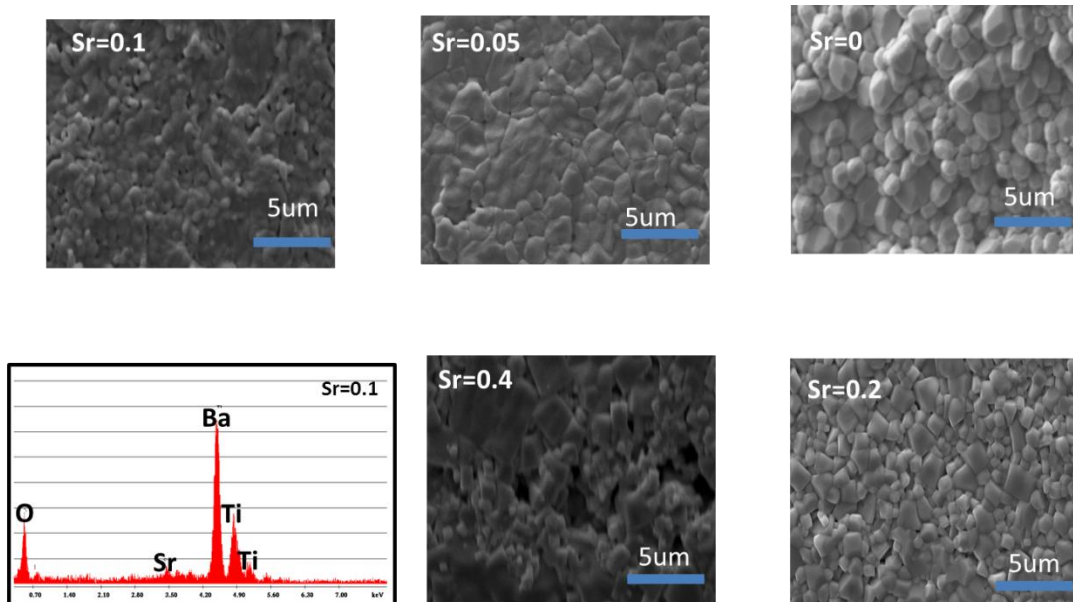
Fig(2).XRD patterns of the  $\text{B1-xSxTiO}_3$  where ( $0 < x \leq 0.4$ ) calcined powder  $1000^\circ \text{C}/3\text{h}$ .

#### 4.2.SEM characterization

The morphology of powders has been investigated by figure (3) show the morphologies, observed by SEM of  $(\text{Ba}_{1-x}\text{Sr}_x)\text{TiO}_3$  ( $x = 0.0, 0.05, 0.1, 0.2$  and  $0.4$  mol%) at  $1200^\circ \text{C}$  for 4 h obtained by sol-gel method. The morphology shows all the compositions exhibit fully dense microstructures with absence completely the porosity exist in the grain boundary, which means the sintering conditions were enough to obtain a fully dense microstructure. For all samples, the morphology exhibits a homogeneous microstructure and uniformly distributed of the grain size. The grain size for all the ceramics are smaller than the grain size for same compositions that are prepared by the solid state reaction technique [19] and this could be the main reason for decreasing the sintering temperature from  $1400^\circ \text{C}$  to  $1200^\circ \text{C}$ . Also, the grain size was observed tend to decrease with increasing the  $\text{Sr}^{2+}$  concentration, and these results confirmed the XRD results. This result may be associated with the substitution of the larger  $\text{Ba}^{2+}$  ion by the smaller  $\text{Sr}^{2+}$  ion and the angle of diffraction are respectively.

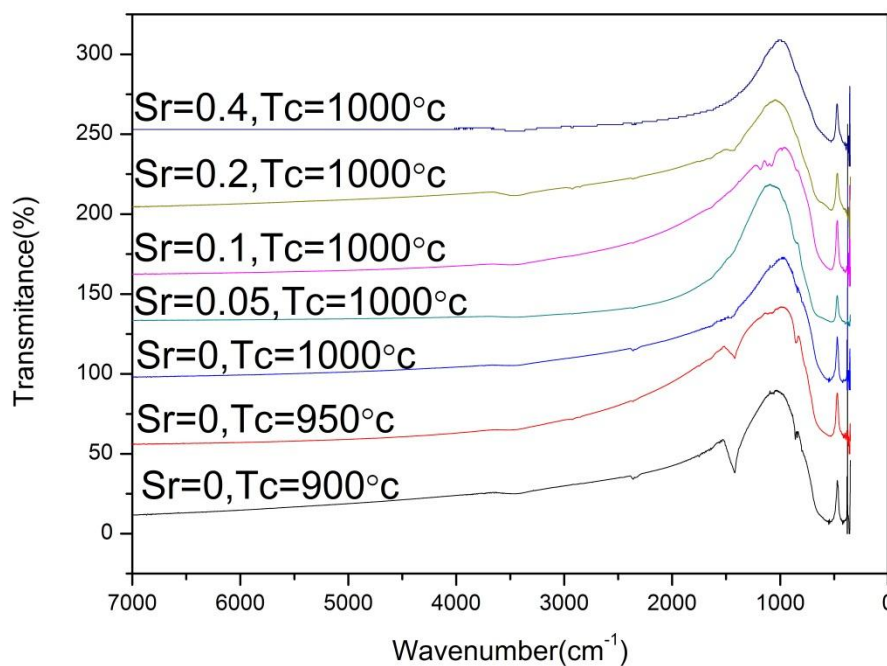
On the other hand, the elementary cell volume is reduced with Sr doping as seen in fig ( ), probably due to the smaller ionic radius of  $\text{Sr}^{2+} = 1.32 \text{ \AA}$  compared to that of  $\text{Ba}^{2+} = 1.49 \text{ \AA}$ .

EDX analysis for BST ceramic  $\text{Sr} = 0.05$  show absence of contamination.



Fig(3).SEM micrographs of the  $B_{1-x}S_xTiO_3$  ceramics sintered at  $1200^\circ\text{C}$  and EDS of  $Sr=0.05$ .

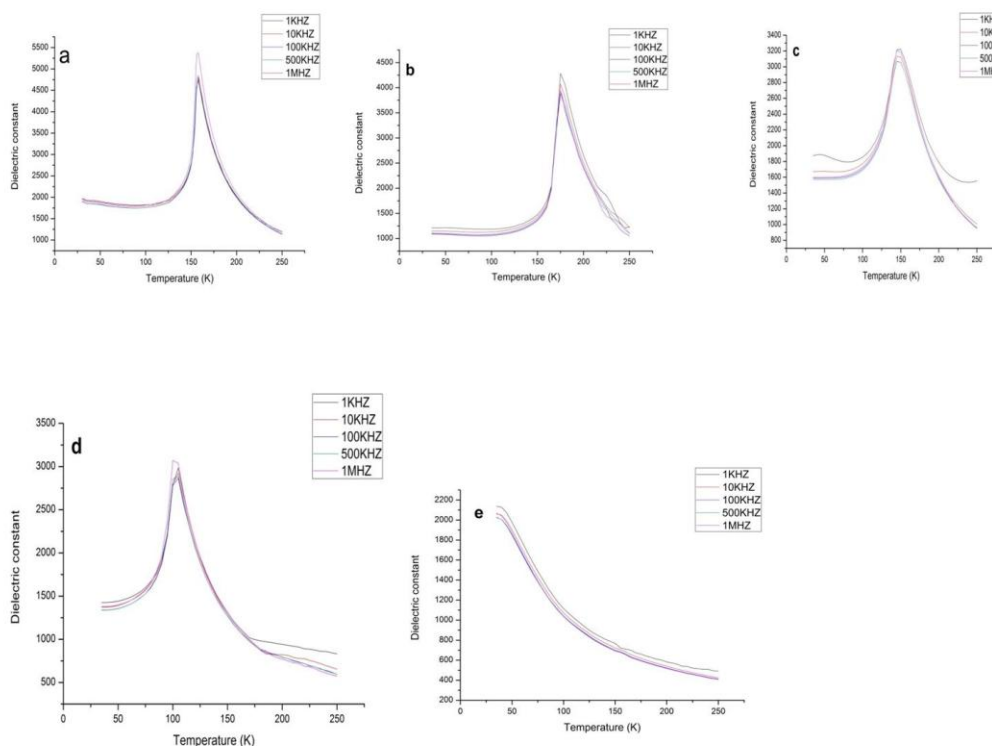
FTIR spectroscopic measurements were used to investigate binding in the prepared Sr doped  $BaTiO_3$  powders. FTIR spectra in the range of  $0-7000\text{cm}^{-1}$ . Two intense bands at  $1430$  and  $1556\text{cm}^{-1}$  are assigned to symmetrical and antisymmetric vibrations respectively (titanium-bound carboxylic groups ( $\text{COO}^-$ ) or stretching of barium)[20,21]. the two broad peaks between  $1000$  and  $1200\text{cm}^{-1}$  can be attributed to isopropyl groups bound to the titanium atoms in a monodentate mode and traces of the carbonate in small amount. At frequency  $900\text{cm}^{-1}$  to  $1700\text{cm}^{-1}$  act the vibration band of the organic (carboxylic) groups decreased with the increase of the strontium doping rate (it disappeared) for  $x=0.4$ , in conformity with XRD results, while the Ti-O absorption peaks become more prominent.



Fig(4).FTIR spectra of the  $B_{1-x}S_xTiO_3$  where ( $0 < x \leq 0.4$ ) calcined powder Sr( $900-1000^\circ\text{C}/3\text{h}$ ).

#### 4.3.DIELECTRIC PROPERTIES:

Temperature dependence of dielectric constant for  $(\text{Ba}_{1-x}\text{Sr}_x)\text{TiO}_3$  ceramics (0,0.1,0.2 and 0.4) at four different frequencies (1KHZ,10KHZ,100KHZ and 500KHZ) are shown in fig (5).the general behavior of permittivity temperature curve for all the compositions can be described as the value of permittivity increased with increasing temperature (curie temperature),then decreased with temperature(paraelectricpase).No clear dielectric dispersion was observed before and after  $T_c$  with changing frequency[22,23].The maximum value of dielectric constant decreases with increasing of  $\text{Sr}^{2+}$  constant ,Sr doping in  $\text{BaTiO}_3$  has been reported to reduce ashift in  $T_c$  from the standard value of  $150^\circ\text{c}$  towards roomtemperature ,this is possibly due to the dominant role played by the smaller particle size and the adsorbed Oxygen at grainboundaries than the dopant ion in lowering the  $T_c$  .In the last case ,the maximum value of permittivity ( $\epsilon_{\text{max}}$ ) decreased with increasing the applied frequency ,this behavior as mentioned above can be interpreted according to the Maxwell-Wanger mechanism .The sample  $\text{Sr}=0.05$  possess the maximum value of permittivity compared to the other compositions . This is because the grain size of the ceramics are decreased significantly with increasing Sr concentration due to the different ionic radius between Sr and Ba ions.

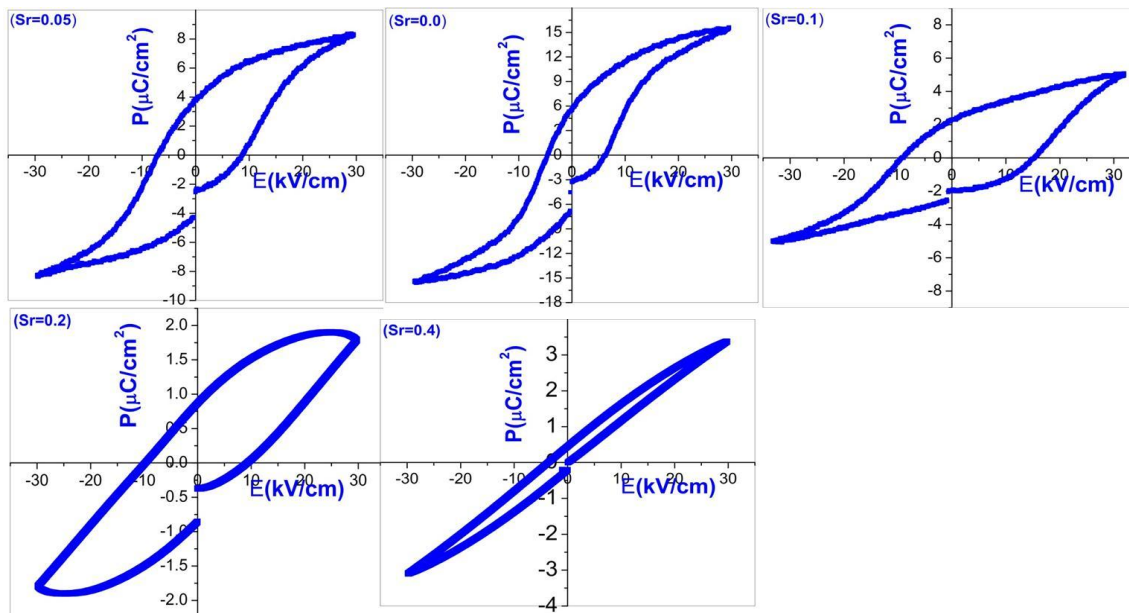


Fig(5).Variation of dielectric constant against temperature for  $\text{Ba}_{1-x}\text{Sr}_x\text{TiO}_3$  where  $(0 < x \leq 0.4)$  ceramics ,at five frequencies

#### 4.4.P-E hysteresis loops:

Fig(6) showed the measured P-E hysteresis loops of the  $\text{Ba}_{1-x}\text{Sr}_x\text{TiO}_3$  ( $x=0.0,0.05,0.1,0.2$  and  $0.4$ ).All samples show the squared hysteresis loops; The spontaneous polarization was calculated to be 6,4,2,1 and  $0.5 \mu\text{c}/\text{cm}^2$  for  $x=0.0,0.05,0.1,0.2$  and  $0.4$  mol% of Sr .The doping of acceptor dopants like Sr causes the creation of the positively charged oxygen vacancy that neutralizes the introduced effective negative charge introduced[24]. Defect dipole suture thus created. These dipoles at the same time behave as elastic dipoles due to the difference in ionic radius of  $\text{Ba}^{2+}$  and  $\text{Sr}^{2+}$ .When an electric field is applied , the onset of spontaneous polarization and strain will tend tonreorient defect dipoles along the polarization direction , so as to reduce their potential energy .polarization direction on each side of adomain wall was fixed by the presence of defects and the walls become more complex to be in motion [25].





Fig(6).P-E hysteresis loops of the  $Ba_{1-x}Sr_xTiO_3$  bipolar ceramics ( $0 < x \leq 0.4$ ) at 1Hz at room temperature

#### IV. CONCLUSION

In this paper we have given the study of the influence of Sr doping on the dielectric properties of  $BaTiO_3$ . The samples were prepared by the recent Sol-gel route. The structural characterization of the various concentrations of BST by XRD reveals a complete crystallization in the pure perovskite structure. Dielectric studies reveal that Sr doping lowers the temperature of the ferro to paraelectric.

#### REFERENCE

- [1]. D.W.Richerson, Second Edition, Marcel Dekker, inc., (1992).
- [2]. N.Nikulin, Mir publishers, Moscow, (1988).
- [3]. Gene H.H. Journal of American Ceramic Society. 1999, 82(4), 797-818.
- [4]. Dey S. K. and Majhi P. International Journal of applied Ceramic Technology. 2005, 2(1):59-63.
- [5]. Zhang Y., Wang G., Zeng T., Liang R., and Dong X. Journal of American Ceramic Society. 2007, 90(4):1327-1330.
- [6]. M.Hu, H.S.Gu, X.C.Sun, J.You and J.Wang, appl.phys.Lett., 88(2006)193120.
- [7]. J.Moon, M.L.Carasso, H.G.Krurup, J.A., Kerchner and J.H.Adair, J.Mater.res., 14(1999)866-875.
- [8]. Un-yeon H., Hyung-Sang P., and Kee-Kahb K. Journal of American Ceramic Society. 2004, 87(12):2168-2174.
- [9]. A.Udomporn, K.Pengpat and S.Ananta, Eur.ceram.Sco., 24(2004)185.
- [10]. H.Hsien-Lin, G.Z.Cao and I.Y.Shen, Sens.Actuat. A phys., 214(2014) 111-119.
- [11]. A.Rujiwatra, N.Thammajak, T.Sarakonsri, R.Wongmaneeung and S.Ananta, J.Cryst.Growth, 289(2006)224.
- [12]. W.Chen and Q.Zhu, Mater.LETT., 61(2007) 3378-3380.
- [13]. J.Fang, J.Wang, L.M.Gan and S.C.Ng, Mater.Lett., 52(2002).
- [14]. S.K.Rout, J.Bera, in: A.P.Tandon (Ed), Allied Publishers Pvt.Ltd., New Delhi. (2004) 3-7.
- [15]. R.M.Mahani, I.k.Battisha, M.Alyb, A.B.AbouHamad, J.Alloys Compd. 508(2010) 354-358.
- [16]. A.Elbaset, F.Abd, T.Lamcharfi, S.Sayouri, M.Aillerie. IREPHY. No.3, 7(2013)287-293.
- [17]. B.D.Cullity, Elements of X-Ray diffraction, Addition-Wesley publishing Company Inc., 1956.
- [18]. E.V.Ramana, F.Figueiras, A.Mahajan, D.M.Tobaldi, B.F.O.Costa, M.P.F.Graca and M.A.Valente. J.Mater.Chem. C, 4(2016)1066-1079.
- [19]. Abd El-razek Mahmoud, Ahmed S. Afify, Amr Mohamed, J.Mater.sci Mater.Electron. 28(2017)11591.
- [20]. N.W.Alock, V.M.Tracy, and T.C.Waddington, J.Chem.Soc., Dalton Trans., (1976)2243-46.
- [21]. E.Sanchez, T.Lopez, R.Gomea, A.Morales and O.Novaro. J.Solid State Chem., 122(1996)309-14.
- [22]. Czekaj, D.; Lisinska-Czekaj, A.; Orkisz, T.; Orkisz, J.; Smalorz, G. J.Eur.Ceram Soc. 2010, 30, 465-470.
- [23]. Wang, X.; Zhang, Y.; Baturin, I.; Liang, T. Mater. Res. Bull. 2013, 48, 3817-3821.
- [24]. S.S.Kim, C.Park, Applied Physics letters, 75(1999) 2554-2556.
- [25]. B.Meyer, D.vanderbilt, Abinitio study of ferroelectric domain walls in  $PbTiO_3$ , Physical Review B, 65(2002)104111.